Control and Cybernetics

vol. **34** (2005) No. 1

The lightest plane structures of a bounded stress level transmitting a point load to a circular support

by

Cezary Graczykowski[1] **and Tomasz Lewiński**[2]

[1] Institute of Fundamental Technological Research
Polish Academy of Sciences
Świętokrzyska 21, 00-049 Warszawa
e-mail: Cezary.Graczykowski@ippt.gov.pl

[2] Warsaw University of Technology
Faculty of Civil Engineering,
Institute of Structural Mechanics
al.Armii Ludowej 16, 00-637 Warsaw, Poland
e-mail: T.Lewinski@il.pw.edu.pl

Abstract: The paper refers to the problem of Michell (1904) of finding the lightest fully stressed structures, composed of possibly infinite number of members, trasmitting a given load to a support forming a circle. The point load can be located within or outside the circle. The known analysis by Hemp (1973) is enhanced here by disclosing the explicit formulae for the weights of the ribs and the interior (fibrous domain). The optimal weight can be found by two manners: by applying the primal integral formula involving the density of the reinforcement or by computing the work of the load on the adjoint displacement. One of the aims of the paper is to show that both these formulae are equivalent. This identity is essential since in the case of point loads the equivalence of the primal and dual formulations has not been proved till now.

The analytically found layouts are confirmed by analysis of trusses (of finite number of joints) approximating the exact Michell-like solutions.

Keywords: Michell cantilevers, layout optimization, minimum weight design.

1. Introduction

Plane Michell structures are exact global solutions to the layout problem of plastic design: find the lightest statically admissible truss or fibrous structure (in which normal stress σ is bounded from both sides by $-\sigma_C$ and σ_T) lying within a given feasible plane domain Ω_0 and supported on a given line.

The problem was originated by Michell (1904). All known plane Michell structures are reported by Hemp (1973), Chan (1967, 1975) and Lewiński et al. (1994). Most of them concern the case of $\sigma_C = \sigma_T = \sigma_{pl}$. Michell structures are important because of the following reasons

i) they refer to the case of the volume being small in the contemporary relaxed formulation of the optimal shape design problem in plane, see Allaire and Kohn (1993)
ii) they are both global and exact solutions
iii) the optimal designs are neither discrete nor continuous: they are fibrous structures reinforced by ribs of finite cross sections.

The problem to be discussed refers to the oldest optimal cantilever problem, see Michell (1904): the support line is of circular shape and $\sigma_C = \sigma_T = \sigma_{pl}$ The case of $\sigma_T \neq \sigma_C$ is difficult and has not been solved till now. For the case of $\sigma_C = \sigma_T$ the solution found by Michell is correct but not complete. Hemp's (1973) analysis is deeper as involving distribution of stress resultants inside the cantilever. It turns out, however, that Hemp did not publish a proof of equivalence of the kinematic and static formulae. One of the motivations of the present paper is to fill up this gap in the literature.

To be more precise, let us recall that the problem considered can be put in terms of stress resultants, as a minimization problem (see (44) below) or can be reformulated to a dual form becoming then a maximization problem (see (46)) expressed in terms of adjoint displacements. In the case of a regular boundary loading, equivalency of these problems was shown in Strang and Kohn (1983). In the original Michell problem the loading is singular, as a point load. For this case the analysis of Strang and Kohn does not apply. In the present paper we put forward both the formulations concerning the point load case and show briefly their equivalence. This theoretical result is confirmed by a direct proof of equivalence of two analytical formulae expressing the volume of the optimal design. This proof is not elementary, see Appendix.

The theoretical solution – composed of two ribs and a fibrous domain – is compared with approximate designs of trusses of finite number of joints. We construct sequences of trusses tending to the ideal design. The speed of convergence of the sequences of the sub-optimal volumes is satisfactory.

Having found the solution discussed above one can solve a similar problem in which the location of application of the point load is located within the given circular domain. This problem is solved analytically and appropriately illustrated.

The paper ends up with an example of optimal design of a wheel subject to a twisting loading. Due to rotational symmetry the problem is fully solvable. This problem should not be confounded up with the optimal design shown in Sec. 17.4 of the book by Cherkaev (2000).

No special conventions are adopted. Before reading the text the reader is asked to remind some formulae referring to orthogonal curvilinear systems. In particular, the book by Novozhilov (1962, 1970) could be helpful. The paper

can be treated as an extension of Sec. 4.6 of the book of Hemp (1973).

Selected results of the present paper were announced by Graczykowski and Lewiński (2003).

2. A point load outside a given circle

The aim of this section is to re-consider the Michell cantilever problem, see Michell (1904) and Hemp (1973, Sec. 4.6). We put an emphasis on the interaction between the fibrous domain and the reinforcing ribs.

2.1. Analysis of equilibrium and computing the volume

We are given a circle of centre A and radius R and a point B outside the circle, of application of the point load $\boldsymbol{P}$. Direction of the force $\boldsymbol{P}$ is given by an angle ϕ_p measured in a counterclockwise direction from the vertical line, see Fig. 1.

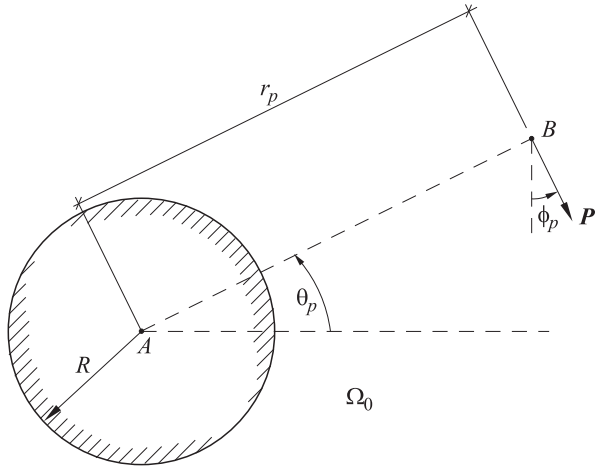

Figure 1. Data for the Michell problem (P_0)

The exterior Ω_0 of the given circle is the feasible domain. Let σ_{pl} represent the admissible stress, common for tension and compression. The Michell problem is formulated as follows

$$(P_0)\quad \left|\begin{array}{l}\text{Find the structure of the smallest volume lying within } \Omega_0,\\ \text{in which } |\sigma| \le \sigma_{pl}, \text{ capable of transmitting the force } \boldsymbol{P}\\ \text{to the boundary of the given circle.}\end{array}\right.$$

The formulation above can be made more restrictive by putting $|\sigma| = \sigma_{pl}$, since the solution should be sought among fully stressed designs.

The solution to (P_0) has been already outlined in Michell (1904) and analyzed in Hemp (1973, Sec. 4.6). However, one can easily note that not all aspects of the solution have been there published. They will be discussed in the sequel.

Let us introduce Cartesian coordinates (x, y) with origin at point A and the polar coordinates (r, θ) such that $x = r\cos\theta$, $y = r\sin\theta$; θ is measured counterclockwise, see Fig. 2.

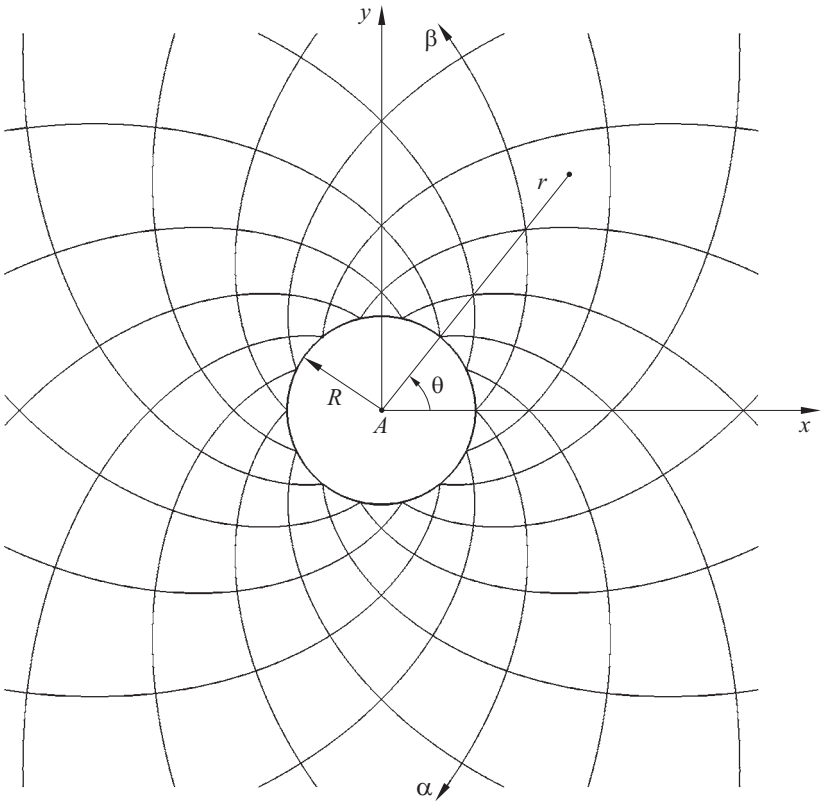

Figure 2. Curvilinear parametrization of the feasible domain

Let us consider a family of logarithmic spirals. The α-lines:

$$x = Re^{2\beta-\theta}\cos\theta\ , \qquad y = Re^{2\beta-\theta}\sin\theta\ , \qquad \theta \in \mathbb{R} \tag{1}$$

where β is fixed and β-lines

$$x = Re^{2\alpha+\theta}\cos\theta\ , \qquad y = Re^{2\alpha+\theta}\sin\theta\ , \qquad \theta \in \mathbb{R} \tag{2}$$

where α is fixed, see Fig. 2. The α- and β-lines form an orthogonal curvilinear

system $\xi^1 = \alpha$, $\xi^2 = \beta$ such that

$$x = Re^{\alpha+\beta}\cos(\beta-\alpha)\ , \qquad y = Re^{\alpha+\beta}\sin(\beta-\alpha) \tag{3}$$

and

$$r = Re^{\alpha+\beta}\ , \qquad \theta = \beta-\alpha \qquad \mathrm{mod}\ (2\pi). \tag{4}$$

The components of the metric tensor of the system (ξ^1, ξ^2) form the matrix $[g_{\lambda\mu}]$, $\lambda, \mu = 1, 2$, such that

$$g_{11} = A^2(\alpha,\beta)\ , \qquad g_{12} = 0\ , \qquad g_{22} = A^2(\alpha,\beta) \tag{5}$$

with

$$A(\alpha,\beta) = \sqrt{2}Re^{\alpha+\beta} \tag{6}$$

Thus, the parametrization (ξ^1, ξ^2) is not only orthogonal, but also isothermal, Vekua (1967, Sec. 57). The lines α and β cut the circles $r = \mathrm{const}$ at angles $\pm\pi/4$. It is known that the solution to the problem (P_0) is described by the parametric lines α and β. This solution is neither discrete nor continuous. It is a certain plate reinforced by ribs transmitting longitudinal forces. The construction of the optimal solution is explained in Fig. 3.

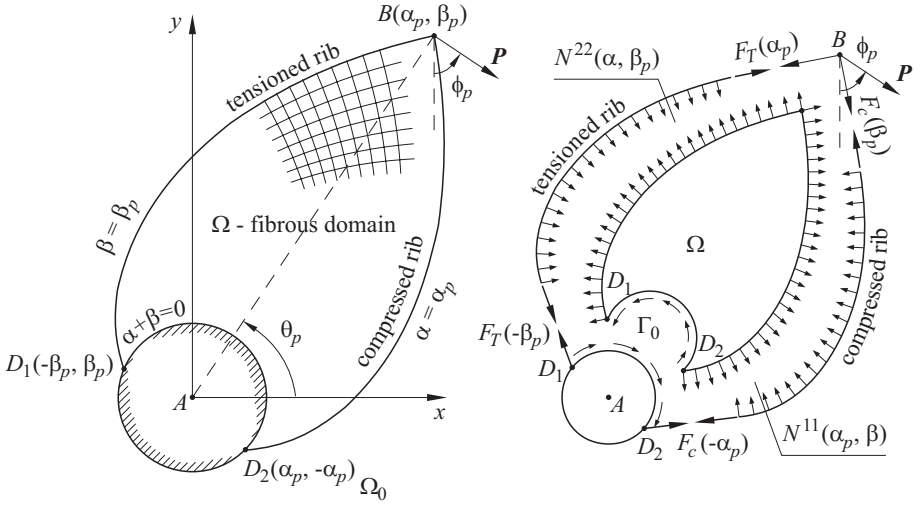

Figure 3. a) Optimal solution, b) decomposition of the optimal solution

It should be done as follows. We find first the (α_p, β_p) coordinates of point B. Then we cut out the domain Ω by the lines: $\beta = \beta_p$, $\alpha = \alpha_p$ and the arc

D_1D_2 with $D_1(-\beta_p, \beta_p)$, $D_2(\alpha_p, -\alpha_p)$ lying on the circle $r = R$. We imagine that the boundary D_1B is reinforced by a cable or a rib with vanishing bending and transverse shear stiffness. This rib will work in tension, transmitting a longitudinal force $F_T(\alpha)$, $-\beta_p \leq \alpha \leq \alpha_p$. The rib D_2B will be compressed by a longitudinal force $F_C(\beta)$, $-\alpha_p \leq \beta \leq \beta_p$. The conditions of equilibrium of the node B imply

$$F_T(\alpha_p) = P_1 \ , \qquad F_C(\beta_p) = P_2 \tag{7}$$

where

$$P_1 = P \sin\left(\frac{\pi}{4} - \theta_p + \phi_p\right) \qquad P_2 = -P \cos\left(\frac{\pi}{4} - \theta_p + \phi_p\right) \tag{8}$$

with $P = |\boldsymbol{P}|$. Here θ_p is the polar coordinate of B. Let us note that

$$P_1 - P_2 = \sqrt{2} P \cos(\theta_p - \phi_p) \ . \tag{9}$$

The optimal structure is composed of three interacting parts: the tensioned rib D_1B, the compressed rib D_2B and the fibrous domain Ω of points (α, β) such that

$$-\beta \leq \alpha \leq \alpha_p \ , \qquad -\alpha_p \leq \beta \leq \beta_p \ , \tag{10}$$

see Fig. 4. The radii of curvature of the lines $\beta = \beta_p$ and $\alpha = \alpha_p$ are given by

$$\rho_T(\alpha) = A(\alpha, \beta_p) \ , \qquad \rho_C(\beta) = A(\alpha_p, \beta) \ . \tag{11}$$

The continuous domain Ω is considered as filled up with fibres following the lines $\xi^1 = \alpha$, $\xi^2 = \beta$. This body has no shear stiffness, hence the tangent stress resultants: $N^{12} = N^{21} = 0$. Other components N^{11}, N^{22} represent stress resultants in the ξ^1 and ξ^2 directions. Here $(N^{\lambda\mu})$ are physical components of the stress resultant tensor, defined as in the plate theory, for plates loaded in plane.

Let us recall the differential equilibrium equations of the rib in tension, see Fig. 3b

$$\frac{dF_T(\alpha)}{ds} = 0 \ , \qquad \frac{F_T(\alpha)}{\rho_T(\alpha)} + N^{22}(\alpha, \beta_p) = 0 \ . \tag{12}$$

where $ds = A(\alpha, \beta_p) d\alpha$. We have taken into account that the rib is not subject to a tangent loading. Thus $F_T(\alpha) = \text{const}$ and by (7) we find $F_T(\alpha) = P_1$, which gives the boundary condition

$$N^{22}(\alpha, \beta_p) = -P_1 A^{-1}(\alpha, \beta_p) \ . \tag{13}$$

Similar arguments lead to $F_C(\beta) = P_2$ and

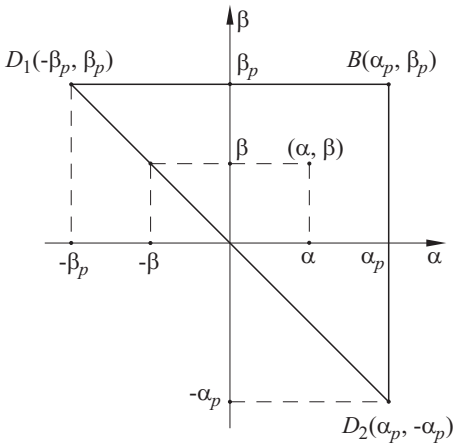

Figure 4. Parameterization of the domain

$$N^{11}(\alpha_p, \beta) = -P_2 A^{-1}(\alpha_p, \beta) \ . \tag{14}$$

Due to the specific form of tensor $\boldsymbol{g}$ and the assumption: $N^{12} = 0$ the differential equilibrium equations for the domain Ω reduce to, see Novozhilov (1962, Ch.2),

$$-\frac{\partial(AN^{11})}{\partial\alpha} + \frac{\partial A}{\partial\alpha} N^{22} = 0 \ , \qquad -\frac{\partial(AN^{22})}{\partial\beta} + \frac{\partial A}{\partial\beta} N^{11} = 0 \tag{15}$$

Due to conditions

$$\frac{\partial A}{\partial\alpha} = A \ , \qquad \frac{\partial A}{\partial\beta} = A \tag{16}$$

it is helpful to introduce new force unknowns

$$T_1 = AN^{11} \ , \qquad T_2 = AN^{22} \tag{17}$$

and re-write (15), (14), (13) in the form

$$-\frac{\partial T_1}{\partial\alpha} + T_2 = 0 \ , \qquad -\frac{\partial T_2}{\partial\beta} + T_1 = 0 \tag{18}$$

$$T_1(\alpha_p, \beta) = -P_2 \ , \qquad T_2(\alpha, \beta_p) = -P_1 \tag{19}$$

Let us note that T_1 and T_2 are of force dimension. Moreover, these fields are fully determined by (18), (19), which discloses that our problem is statically determinate.

REMARK 2.1 *Problem* (P_0) *can be posed in a discrete setting: find the lightest truss (of finite number of members and joints) satisfying the given conditions. One can prove that among the optimal designs at least one is statically determinate, see Achtziger (1997). To find the smallest weight one could confine optimization to the class of statically determinate trusses. Looking at (12)-(14), (18), (19) we note that our problem is fully statically determinate. This property holds here thus showing that our optimal structure could be viewed as a singular truss of infinite number of members and joints.*

To solve (18), (19) we use the Riemann method, see Hemp (1973, Sec. 4.6). Let us introduce the family of functions

$$G_n(\alpha,\beta) = \left(\frac{\alpha}{\beta}\right)^{\frac{n}{2}} I_n\left(2\sqrt{\alpha\beta}\right) \tag{20}$$

$n = 0, 1, 2$; $I_n(\cdot)$ is the modified Bessel function, or

$$I_n\left(2\sqrt{\alpha\beta}\right) = (\alpha\beta)^{\frac{n}{2}} \sum_{k=0}^{\infty} \frac{(\alpha\beta)^k}{k!(k+n)!} \ . \tag{21}$$

The following identities hold, see Lewiński et al. (1994a, b),

$$\frac{\partial G_n(\alpha,\beta)}{\partial\alpha} = G_{n-1}(\alpha,\beta) \ , \qquad \frac{\partial G_n(\alpha,\beta)}{\partial\beta} = G_{n+1}(\alpha,\beta) \tag{22}$$

where $G_{-1}(\alpha,\beta) = G_1(\beta,\alpha)$. Let us recall the Riemann result. If a function $w(\alpha,\beta)$ is defined for

$$\theta_1 \le \alpha \le \lambda \ ; \qquad \theta_2 \le \beta \le \mu \tag{23}$$

and satisfies

$$\frac{\partial^2 w}{\partial\alpha\partial\beta} - w = 0 \tag{24}$$

then w is given directly by the Riemann formula

$$\begin{aligned} w(\lambda,\mu) = {} & w(\theta_1,\theta_2)G_0(\lambda-\theta_1,\mu-\theta_2) + \\ & + \int_{\theta_1}^{\lambda} G_0(\lambda-\alpha,\mu-\theta_2)\frac{\partial w(\alpha,\theta_2)}{\partial\alpha}d\alpha + \\ & + \int_{\theta_2}^{\mu} G_0(\lambda-\theta_1,\mu-\beta)\frac{\partial w(\theta_1,\beta)}{\partial\beta}d\beta \ . \end{aligned} \tag{25}$$

The formula above along with (22) make it possible to solve (18)-(19). The results are

$$\begin{aligned} T_1(\alpha,\beta) &= -P_2 G_0(\alpha_p-\alpha,\beta_p-\beta) + P_1 G_1(\alpha_p-\alpha,\beta_p-\beta) \\ T_2(\alpha,\beta) &= -P_1 G_0(\alpha_p-\alpha,\beta_p-\beta) + P_2 G_1(\beta_p-\beta,\alpha_p-\alpha) \ . \end{aligned} \tag{26}$$

The volume of fibres within the elementary area $dS = A^2 d\alpha\, d\beta$ is expressed in terms of N_I and N_{II} (or principal values of tensor $\boldsymbol{N}$) by, see Lewiński and Telega (2000, Eq. 29.1.11) for a physical explanation,

$$dV = \frac{1}{\sigma_{pl}} \left(|N_I| + |N_{II}|\right) dS \ . \tag{27}$$

Here $N_I = N^{11}$ and $N_{II} = N^{22}$. Thus, we have

$$dV = \frac{1}{\sigma_{pl} A} \left(|T_1| + |T_2|\right) dS \ . \tag{28}$$

The function

$$h(\alpha, \beta) = \frac{1}{\sigma_{pl}} \left(|T_1(\alpha, \beta)| + |T_2(\alpha, \beta)|\right) A^{-1}(\alpha, \beta) \tag{29}$$

measures the density of fibres. Following Hemp (1973) this function will be called an effective thickness of the fibrous domain Ω. Substitution of (6), (26) gives

$$\begin{aligned} h(\alpha, \beta) = \frac{1}{\sqrt{2}\sigma_{pl} R} e^{-(\alpha+\beta)} \left[(P_1 - P_2) G_0(\alpha_p - \alpha, \beta_p - \beta) + \right. \\ \left. + \ P_1 G_1(\alpha_p - \alpha, \beta_p - \beta) - P_2 G_1(\beta_p - \beta, \alpha_p - \alpha)\right] \end{aligned} \tag{30}$$

since $|T_2| = -T_2$. The volume of the fibrous domain equals, see Fig. 4,

$$V_F = \int_{-\alpha_p}^{\beta_p} \int_{-\beta}^{\alpha_p} h(\alpha, \beta) A^2(\alpha, \beta) d\alpha\, d\beta \ . \tag{31}$$

The integral identity (A1) makes it possible to express V_F as follows

$$V_F = \frac{\sqrt{2} R}{\sigma_{pl}} (P_1 - P_2) \mathcal{J}(\alpha_p, \beta_p) \tag{32}$$

where

$$\begin{aligned} \mathcal{J}(\alpha_p, \beta_p) = \int_{-\alpha_p}^{\beta_p} \int_{-\beta}^{\alpha_p} e^{\alpha+\beta} \left[G_0(\alpha_p - \alpha, \beta_p - \beta) + \right. \\ \left. + \ G_1(\alpha_p - \alpha, \beta_p - \beta)\right] d\alpha\, d\beta \ . \end{aligned} \tag{33}$$

The identity (A2) and (9) give the final result

$$V_F = \frac{2PR}{\sigma_{pl}} \left\{\left[(\alpha_p + \beta_p) - 1\right] e^{\alpha_p + \beta_p} + 1\right\} \cos(\theta_p - \phi_p) \ . \tag{34}$$

Let us compute now the volume of the tensioned rib. Its cross section is P_1/σ_{pl}, hence the volume is expressed by

$$V_{RT} = \frac{P_1}{\sigma_{pl}} \int_{-\beta_p}^{\alpha_p} A(\alpha, \beta_p) d\alpha \tag{35}$$

or

$$V_{RT} = \frac{\sqrt{2} R P_1}{\sigma_{pl}} \left(e^{\alpha_p + \beta_p} - 1 \right) \ . \tag{36}$$

In a similar way we find the volume of the compressed rib

$$V_{RC} = \frac{-\sqrt{2} R P_2}{\sigma_{pl}} \left(e^{\alpha_p + \beta_p} - 1 \right) \ . \tag{37}$$

The total volume of the ribs equals $V_R = V_{RT} + V_{RC}$. By using (9), (36), (37) we arrive at

$$V_R = \frac{2PR}{\sigma_{pl}} \left(e^{\alpha_p + \beta_p} - 1 \right) \cos(\theta_p - \phi_p) \ . \tag{38}$$

By adding (34) and (38) we find the total volume of the optimal structure $V = V_F + V_R$ or

$$V = \frac{2PR}{\sigma_{pl}} (\alpha_p + \beta_p) e^{\alpha_p + \beta_p} \cos(\theta_p - \phi_p) \ . \tag{39}$$

If (r_p, θ_p) are polar coordinates of B we can rearrange (39) to the form

$$V = \frac{2P}{\sigma_{pl}} r_p \ln \left(\frac{r_p}{R} \right) \cos(\theta_p - \phi_p) \tag{40}$$

which directly links the volume with the data of the problem, see Fig. 1.

We note that the volume V can be expressed as a sum of the surface and line integrals

$$\sigma_{pl} V = \int_\Omega \left(|N_I| + |N_{II}| \right) dS + \int_{\partial\Omega \setminus \Gamma_0} |F| ds \tag{41}$$

where $\Gamma_0 \subset \partial\Omega_0$ is a part of a boundary of the circle. Here $F = F(s)$ represents the longitudinal force in the rib reinforcing the free boundary. The force fields: $\boldsymbol{N} = (N^{\lambda\mu})$ within Ω and F along $\partial\Omega$ equilibrate the given point load at B. We say that $\boldsymbol{N}$ and F are statically admissible. This condition can be put in a variational form as follows. Let $\overline{\boldsymbol{u}} = (\overline{u}_x, \overline{u}_y)$ be a sufficiently regular field in Ω_0, vanishing on Γ_0. Then we say that $\overline{\boldsymbol{u}}$ is kinematically admissible and write $\overline{\boldsymbol{u}} \in \mathcal{U}$. Let $\overline{u}_n$, $\overline{u}_\tau$ be normal and tangent components of $\overline{\boldsymbol{u}}$ along $\partial\Omega$. Let s parametrize $\partial\Omega$ and $\rho(s)$ represent a radius of curvature of $\partial\Omega$. Let

$\boldsymbol{\varepsilon}(\overline{\boldsymbol{u}})$ represent the strain field associated with $\overline{\boldsymbol{u}}$, defined as in linear elasticity theory. We introduce a set $\Sigma(\Omega)$ of fields $\widetilde{\boldsymbol{N}} \in L^2(\Omega, \mathbb{E}^2_s)$, $\widetilde{F} \in L^2(\partial\Omega, \mathbb{R})$ such that $\mathrm{div}\widetilde{\boldsymbol{N}} \in L^2(\Omega, \mathbb{R}^2)$, $d\widetilde{F}/ds \in L^2(\partial\Omega, \mathbb{R})$ and

$$\int_\Omega \widetilde{\boldsymbol{N}} : \boldsymbol{\varepsilon}(\overline{\boldsymbol{u}}) dS + \int_{\partial\Omega\setminus\Gamma_0} \widetilde{F}\lambda(\overline{\boldsymbol{u}}) ds = \boldsymbol{P}\cdot\overline{\boldsymbol{u}}(B) \qquad \forall\ \overline{\boldsymbol{u}} \in \mathcal{U} \tag{42}$$

where

$$\lambda(\overline{\boldsymbol{u}}) = \frac{d\overline{u}_\tau}{ds} + \frac{\overline{u}_n}{\rho} \tag{43}$$

represents a relative elongation of the boundary fibre. The set $\Sigma(\Omega)$ comprises all statically admissible pairs $(\widetilde{\boldsymbol{N}}, \widetilde{F})$.

Let us treat the right-hand side of (41) as a value of a functional $I_{\widetilde{\Omega}}(\widetilde{\boldsymbol{N}}, \widetilde{F})$ for $\widetilde{\Omega} = \Omega$, $\widetilde{\boldsymbol{N}} = \boldsymbol{N}$, $\widetilde{F} = F$. We state now the conjecture

$$\sigma_{pl}V = \inf\left\{ I_{\widetilde{\Omega}}(\widetilde{\boldsymbol{N}}, \widetilde{F}) \;\middle|\; (\widetilde{\boldsymbol{N}}, \widetilde{F}) \in \Sigma(\widetilde{\Omega})\ , \quad \widetilde{\Omega} \subset \Omega_0 \right\}\ . \tag{44}$$

Thus we claim that the structure found is the lightest among all which equilibrate the load $\boldsymbol{P}$ and transmit this load to a given circular support.

The conjecture (44) will be justified by duality arguments put forward in the sequel.

2.2. Dual formulation

Let us fix $\widetilde{\Omega}$. We combine (41)-(44) to find a saddle-point problem

$$\begin{aligned}\sigma_{pl}V = \inf_{(\widetilde{\boldsymbol{N}},\widetilde{F})\in\Sigma(\widetilde{\Omega})}\ \sup_{\overline{\boldsymbol{u}}\in\mathcal{U}} \Big\{ I_{\widetilde{\Omega}}(\widetilde{\boldsymbol{N}}, \widetilde{F}) + \boldsymbol{P}\cdot\overline{\boldsymbol{u}}(B)\ - \int_{\widetilde{\Omega}} \widetilde{\boldsymbol{N}} : \boldsymbol{\varepsilon}(\overline{\boldsymbol{u}}) dS + \\ - \int_{\widetilde{\gamma}} \widetilde{F}\lambda(\overline{\boldsymbol{u}}) ds \Big\}\end{aligned} \tag{45}$$

where $\widetilde{\gamma} = \partial\widetilde{\Omega}\setminus\Gamma_0$. The duality arguments by Strang and Kohn (1983) apply here. Thus we can interchange the operators inf and sup and reduce the problem to

$$\sigma_{pl}V = \sup\{\, \boldsymbol{P}\cdot\overline{\boldsymbol{u}}(B) \mid \overline{\boldsymbol{u}} \in \mathcal{U}\,, \quad \boldsymbol{\varepsilon}(\overline{\boldsymbol{u}}) \in \mathbb{B}\,, \quad |\lambda(\overline{\boldsymbol{u}})| \le 1 \quad \text{on} \quad \widetilde{\gamma}\}\,, \tag{46}$$

see also Lewiński and Telega (2001). Here $\mathbb{B}$ represents a locking locus:

$$\mathbb{B} = \left\{ \boldsymbol{\varepsilon} \in \mathbb{E}^2_s \;\middle|\; |\varepsilon_I| \le 1\ , \quad |\varepsilon_{II}| \le 1 \right\}\ .$$

Note that the case of $|\varepsilon_I| = 1$, $|\varepsilon_{II}| = 1$ implies $|\lambda(\overline{\boldsymbol{u}})| = 1$ along $\widetilde{\gamma}$ and can only be fulfilled if

a) the boundary $\widetilde{\gamma}$ follows one of trajectories of principal strain $\boldsymbol{\varepsilon}(\overline{\boldsymbol{u}})$
b) $\widetilde{\gamma}$ is tangent to trajectories of $\boldsymbol{\varepsilon}(\overline{\boldsymbol{u}})$.

In the present paper we confine our consideration to the case

$$\varepsilon_I = 1 \ , \qquad \varepsilon_{II} = -1 \qquad \text{in} \quad \widetilde{\Omega} \tag{47}$$

and, consequently

$$|\lambda(\overline{\boldsymbol{u}})| = 1 \qquad \text{on} \quad \widetilde{\gamma} \tag{48}$$

Let us note that formulation (46) becomes independent of $\widetilde{\Omega}$. Indeed, the conditions (47) can be imposed within Ω_0 while the boundary $\widetilde{\gamma}$ should be chosen as composed of trajectories of ε_I, ε_{II} having a cross section at point B. Thus we rearrange (46) to the form

$$\sigma_{pl} V = \sup_{\substack{\overline{\boldsymbol{u}} \in \mathcal{U} \\ \varepsilon_I(\overline{\boldsymbol{u}})=1 \, , \ \varepsilon_{II}(\overline{\boldsymbol{u}})=-1}} \boldsymbol{P} \cdot \overline{\boldsymbol{u}}(B) \tag{49}$$

since the condition $|\lambda(\overline{\boldsymbol{u}})| = 1$ is satisfied automatically, if the boundary $\widetilde{\gamma}$ is appropriately chosen. The power of the formulation (49) lies in its independence of $\widetilde{\Omega}$. The virtual field $\overline{\boldsymbol{u}}$ concerns the whole domain Ω_0 and Ω will occur as being cut out along trajectories $\varepsilon_I = 1$, $\varepsilon_{II} = -1$ intersecting at point B.

Let us try to satisfy the conditions (47) within the $\xi^1 = \alpha$, $\xi^2 = \beta$ parameterization introduced in Sec. 2.1. Due to their isothermal property the deformations $(\varepsilon_{\lambda\mu})$ are expressed in terms of displacements u (tangent to α-lines) and v (tangent to β-lines) by the formulae, see Novozhilov (1970) and Mazurkiewicz (1995),

$$\begin{aligned} \varepsilon_{11} &= \frac{1}{A}\left(\frac{\partial u}{\partial \alpha} + \frac{1}{A}\frac{\partial A}{\partial \alpha} v\right) \\ 2\varepsilon_{12} &= \frac{\partial}{\partial \alpha}\left(\frac{v}{A}\right) + \frac{\partial}{\partial \beta}\left(\frac{u}{A}\right) \ , \qquad \varepsilon_{22} = \frac{1}{A}\left(\frac{\partial v}{\partial \beta} + \frac{1}{A}\frac{\partial A}{\partial \beta} u\right) \ . \end{aligned} \tag{50}$$

Let us note that the deformations associated with the displacement fields

$$u(\alpha, \beta) = (\alpha + \beta) A(\alpha, \beta) \ , \qquad v(\alpha, \beta) = -u(\alpha, \beta) \tag{51}$$

where $A(\alpha, \beta)$ is given by (6), see (16), are homogeneous

$$\varepsilon_{11} = 1 \ , \qquad \varepsilon_{12} = 0 \ , \qquad \varepsilon_{22} = -1 \tag{52}$$

and $u = 0$, $v = 0$ along the circular boundary of Ω_0. Thus $\overline{\boldsymbol{u}} = (u, v) \in \mathcal{U}$ and (47) are satisfied in Ω_0. Here α and β lines are trajectories of principal strains.

The formulae (51) can be rewritten to the form

$$u/R = \sqrt{2} \frac{r}{R} \ln\left(\frac{r}{R}\right) \ , \qquad v = -u \ . \tag{53}$$

We see that (u, v) do not depend on $\theta = \beta - \alpha$. The radial and circumferential components are

$$u_r = 0 \ , \qquad u_\theta = -2r \ln\left(\frac{r}{R}\right) \ . \tag{54}$$

Let us compute the virtual work of $\boldsymbol{P}$

$$\boldsymbol{P} \cdot \overline{\boldsymbol{u}}(B) = P_1 u(B) + P_2 v(B) \ . \tag{55}$$

By (51) we have

$$\boldsymbol{P} \cdot \overline{\boldsymbol{u}}(B) = (P_1 - P_2) u(B)$$

and by (9) we find

$$\boldsymbol{P} \cdot \overline{\boldsymbol{u}}(B) = 2P \cos(\theta_p - \phi_p) r_p \ln\left(\frac{r_p}{R}\right) \tag{56}$$

which, by (49), gives the previous result (40)

The above identity shows the equivalency of (44) and (46) and confirms that the structure analyzed in Sec. 2.1 is one of optimal solutions. No other structure, with stresses satisfying $|\sigma| \leq \sigma_{pl}$, transmitting the force $\boldsymbol{P}$ to the circular support can be lighter.

2.3. Structure of the optimal solution

The passage from (45) to (46) teaches us that the bars (fibres) must follow trajectories of principal strains, see Strang and Kohn (1983) and Rozvany (1976). Thus the fibres lie along the net of lines α and β and the boundary fibres become ribs of finite cross sections. The net is orthogonal. The fibres are fully stressed such that $|\sigma| = \sigma_{pl}$. The stresses should not be mixed up with the stress resultants N^{11}, N^{22} which are distributed non-homogeneously, according to (17) and (26). The fibres do not sustain shear.

The ribs hinder the fibrous domain from being broken up. They equilibrate the stress resultants normal to the edges. The boundary equilibrium is possible due to curving of the ribs, see Eq. $(12)_2$. If the ribs were straight and still incapable of sustaining the transverse shear forces, the flux of normal stresses could not be arrested. Thus, the lack of shear stiffness brings about appearance of curved boundaries. The second role of the ribs is to carry a concentrated load and change its action into normal loading applied along the curved boundaries of the fibrous domain. Let us stress that the joint at B is safely equilibrated, as would be a joint of a truss.

Let us add that this pseudo-truss is statically determinate. The static analysis can be performed provided that it is done in an appropriate sequence. One should start from the equilibrium equations of the node B, which gives the forces in the ribs. Having their curvature we find the normal loading. This loading

determines the force fields T_1, T_2, since they are governed by the hyperbolic equation (24). Having found T_1, T_2 we compute reactions along the arc D_1D_2.

The shape of the optimal design depends on the ratio r_p/R or on the values α_p and β_p. If $\alpha_p = \beta_p = \pi/4$ the interval D_1D_2 is orthogonal to AB. For $\alpha_p = \beta_p = \pi/2$ we have $D_1 = D_2$. For greater α_p, β_p the tensioned rib will intersect with the compressed rib. For greater values of α_p, β_p these ribs wound around the circle. This clears up why V tends to infinity if $r_p = \text{const}$ and $R \to 0$. In fact, the ribs have constant cross sections and their lengths increase to infinity. We conclude that one cannot fix a cantilever at a point.

Distribution of the effective thickness h is symmetric if $\boldsymbol{P}$ is orthogonal to AB. Then $F_T = -F_C$. The force $\boldsymbol{P}$ can be directed within the angle: $-\dfrac{\pi}{4} + \theta_p < \phi_p < \dfrac{\pi}{4} + \theta_p$. In the limit cases $F_T = 0$ or $F_C = 0$.

Distribution of the function $h(\alpha, \beta)$ depends on the ratio r_p/R and on ϕ_p, see Figs. 5-7.

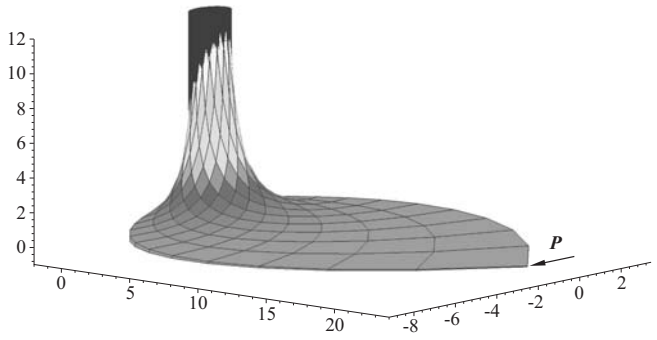

Figure 5. Density of fibres $h(\alpha, \beta)$. Case: $r_p/R = 23.14$, $\phi_p = 0^\circ$

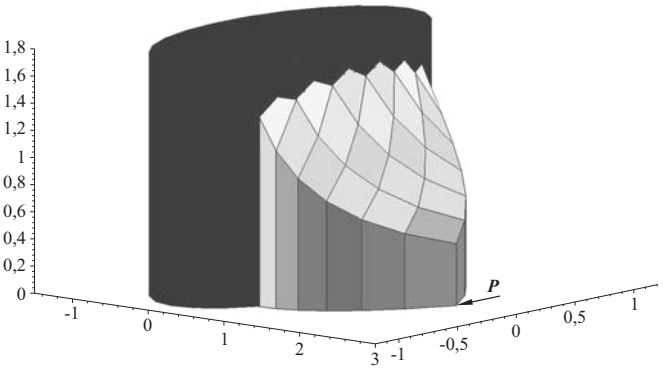

Figure 6. Density $h(\alpha, \beta)$. Case: $r_p/R = 2.19$, $\phi_p = 0^\circ$

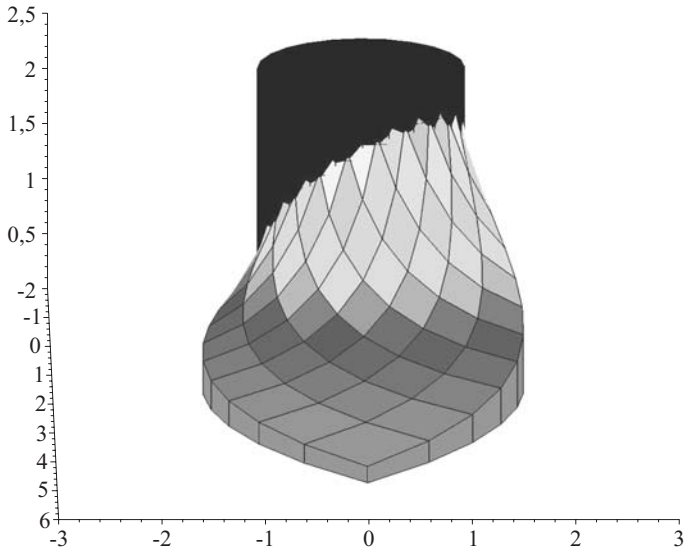

Figure 7. Density $h(\alpha, \beta)$. Case: $r_p/R = 4.81$, $\phi_p = 45^\circ$

Let us consider the ratio V_R/V. By (38)-(40) we have

$$V_R/V = \frac{e^{\alpha_p+\beta_p} - 1}{e^{\alpha_p+\beta_p}(\alpha_p + \beta_p)} \ . \tag{57}$$

We note that $V_R/V \to 1$ if $\alpha_p + \beta_p \to 0$. Therefore, if B tends to the circular boundary, the structure tends to a two-bar design, which is an exact design if the supporting line is straight.

2.4. Approximations by trusses of finite number of joints

The discrete-continuous solutions found above can be compared with discrete or truss designs with finite number of joints and bars. The bars will be placed along trajectories of adjoint principal strains. All the trusses considered will be statically determinate. The cross-sections are selected such that the stresses in each bars are equal to the given limit value.

The greater number of bars the lighter the trusses. The decay of the truss weight is the most clearly visible in the case of a cantilever truss supported on a whole circle. For the considered sequence of sub-optimal designs (see Fig. 8) the decay of the weight equals 37.4%. The external bars play the role of the reinforcing ribs. The internal bars replace the fibrous domain. The weights of the internal bars and boundary bars depend on the number of all bars, see Figs. 8 and 9.

We observe that if the number of bars increases then the total weight decreases, the weight of both the external bars decreases and the weight of internal

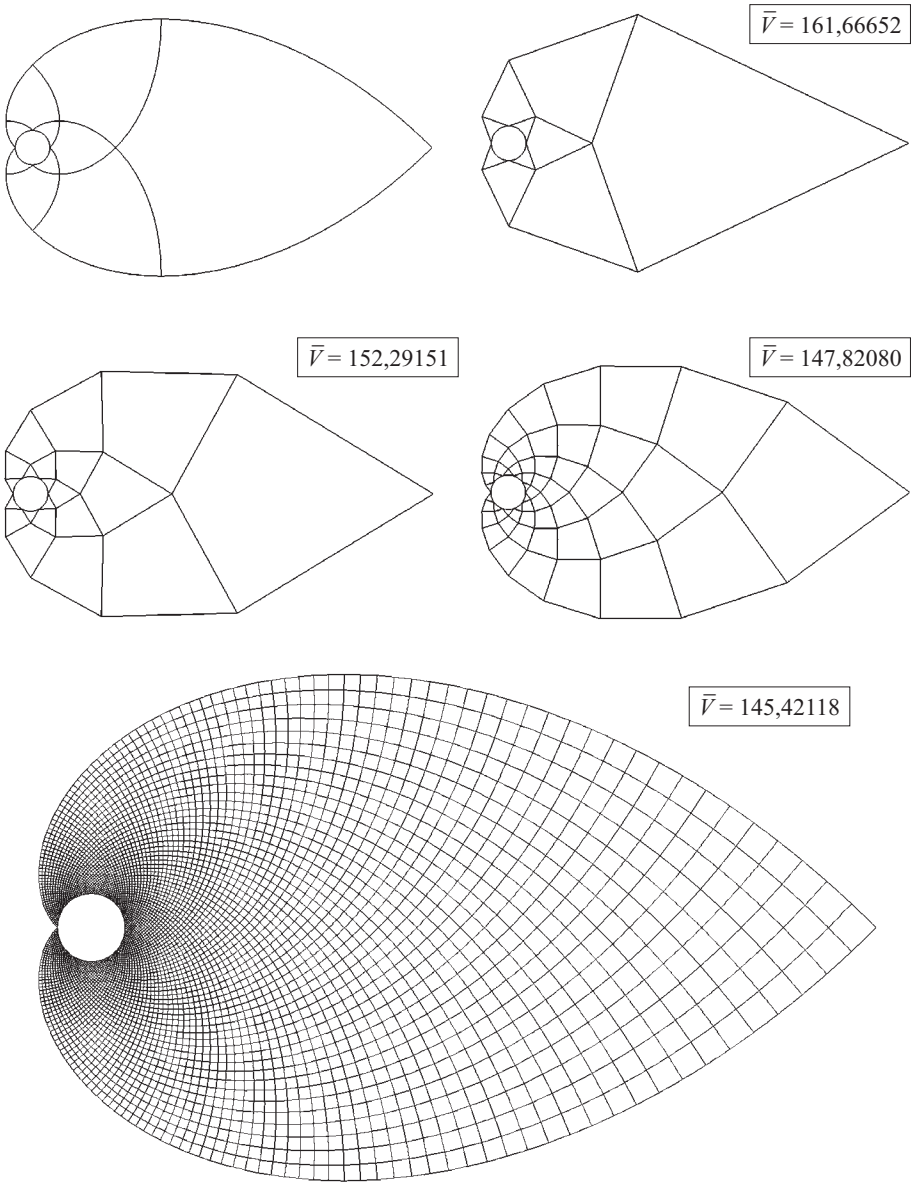

Figure 8. Sequence of trusses approximating the optimal Michell cantilever supported on the whole circumference of the circular support. The first figure shows the Hencky net for fixing the joints of the 10-joint truss. Other trusses are constructed in a similar way. The non-dimensional volumes $\overline{V} = V\sigma_{pl}/PR$ are given beside the trusses

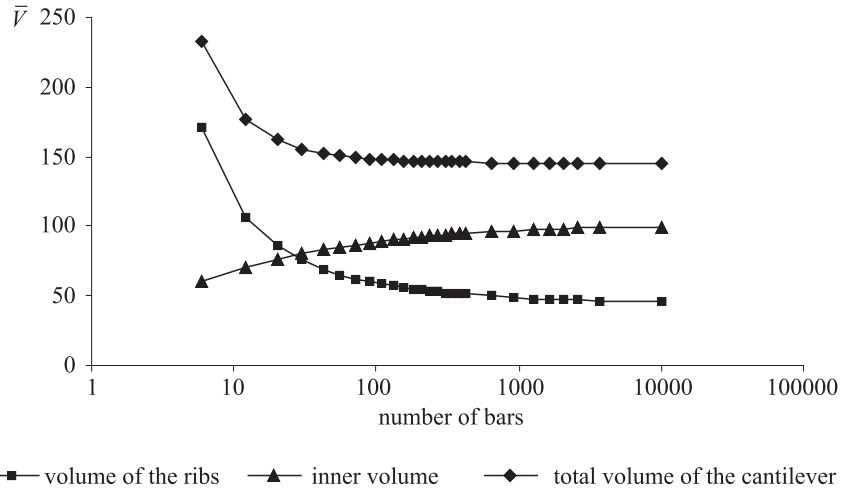

Figure 9. Non-dimensional truss volume $\overline{V} = V\sigma_{pl}/PR$ versus the number of bars of trusses of Fig. 8

bars increases. The truss composed of 10100 bars looks similar to the optimum design by Michell. Its volume equals $145.421PR\rho/\sigma_{pl}$, while the volume of the Michell truss equals $145.397PR\rho/\sigma_{pl}$. The weight of external bars is equal to 68.7% of the total weight, while the corresponding ratio for the Michell solution equals 69.5%. The longitudinal forces along the external bars have almost uniform distribution, which resembles the result for the exact solution where this force is constant within the ribs.

If the truss is loaded by a force directed at angle 30° from the vertical line the weight of the tensioned bars is greater than the weight of the compressed bars. The division of bars into external and internal bars holds also in this case.

Consider the trusses supported on a half of a circle, see Fig. 10.

In this case the decrease of the weight with the increasing number of the bars is not so visible. The simplest truss carrying the point load composed of 6 bars is 11.1% heavier than the optimal design. A greater change is seen as regards division of the weight into the weight of external bars and internal bars (Fig. 11).

In the simplest truss the weight of the internal part is 20.8% of the total weight, in the case of the truss composed of 3660 bars this ratio is 48.52%, while for the optimal design this ratio equals 49.57%. The weight of the truss tends now very rapidly to the optimal value and the variation of the longitudinal force in the external bars is smaller. This is due to a simpler geometry of this truss.

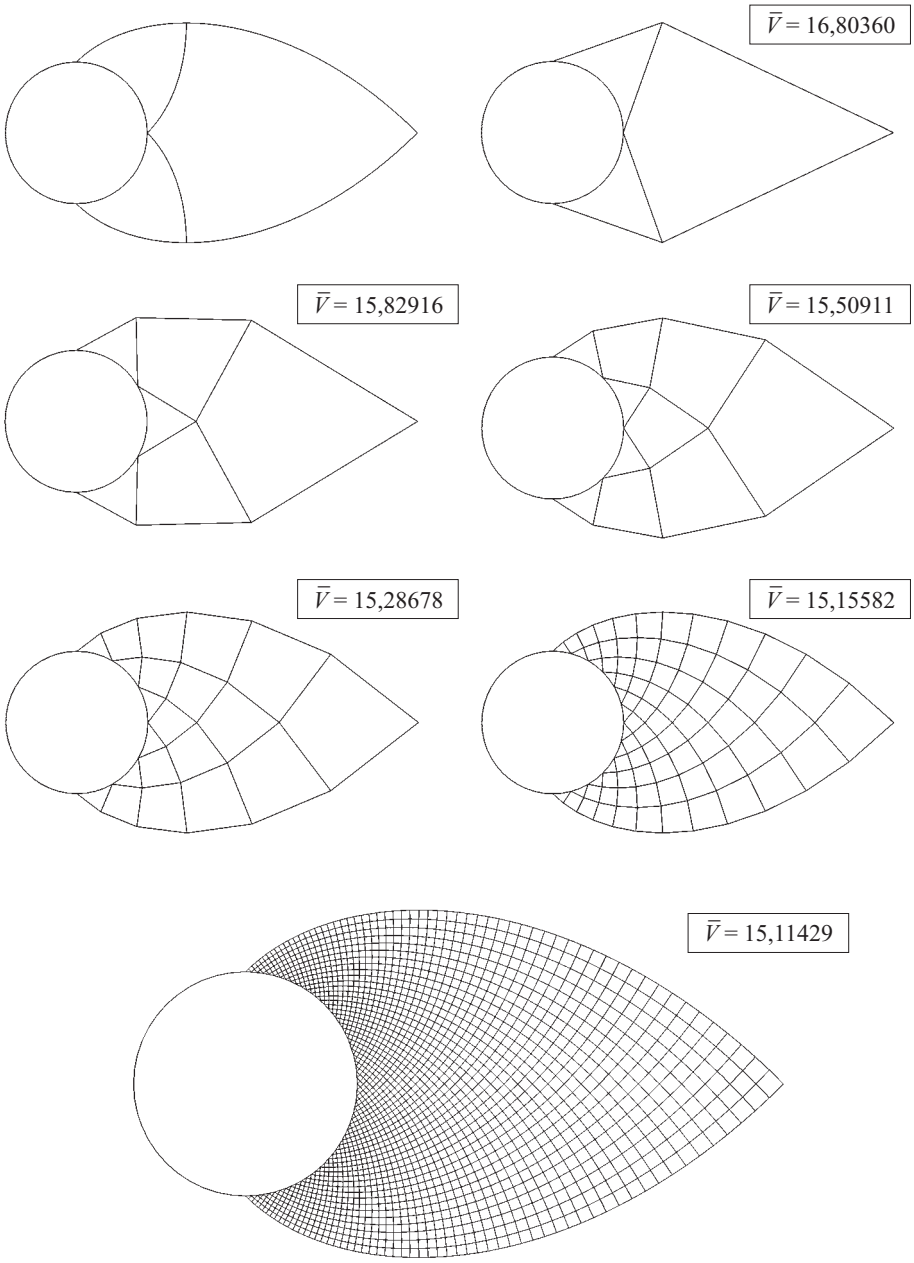

Figure 10. Sequence of trusses supported on one half of the circumference of the support. The first figure shows the auxiliary Hencky net

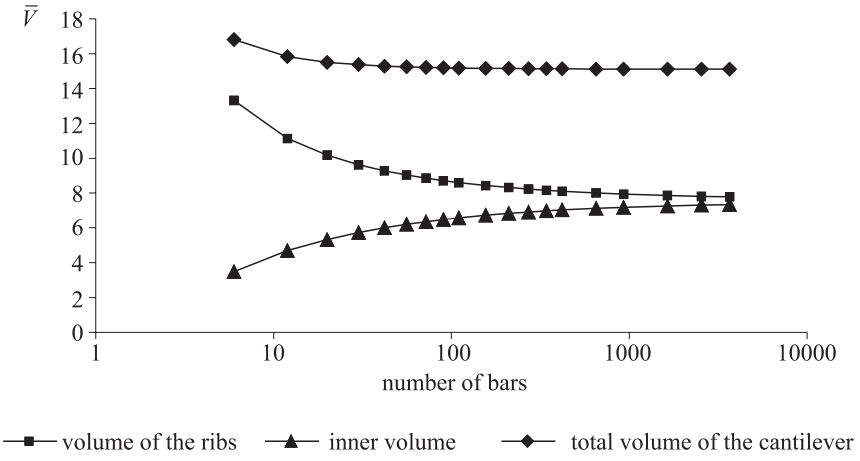

Figure 11. Non-dimensional truss volume for trusses of Fig. 10

Consider now the trusses supported on a quarter of a circle, see Fig. 12. The simplest truss, composed of 6 bars, has the weight 2% greater than the weight of the Michell design. Depending on the number of bars the weight of internal bars varies from 14 to 31% of the total volume.

The examples above show that if the distance of the force to the boundary of the circle diminishes the curvature of the Hencky net is smaller and smaller. The concentrated load is then mainly transmitted by the external bars and the role of internal bars becomes marginal. Thus the main part of the weight is the weight of external bars. If the force is located very near the circular boundary then the shape of the boundary is almost straight and the optimal design tends to the two-bar design. A sequence of suboptimal designs is given in Fig. 13.

3. A point load inside a given circle

Let us assume that the interior of the circle is the feasible domain of the optimal design problem similar to that considered in the previous section. The supporting line will be a part of the circumference of the circle. The point load will be directed downwards, hence the fibres lying along the α-lines will be now compressed and the fibres lying along the β-lines will be tensioned. As before the optimal structure occurs to be fibrous, reinforced by two boundary ribs, one in compression and one in tension. The values of the longitudinal forces in the ribs can be found by the equilibrium conditions of point of application of the force. The longitudinal forces in the ribs are given by the formulae

$$F_T = P\sin\left(\frac{\pi}{4} - \theta + \phi_p\right) \ , \qquad F_C = -P\cos\left(\frac{\pi}{4} - \theta + \phi_p\right) \ . \tag{58}$$

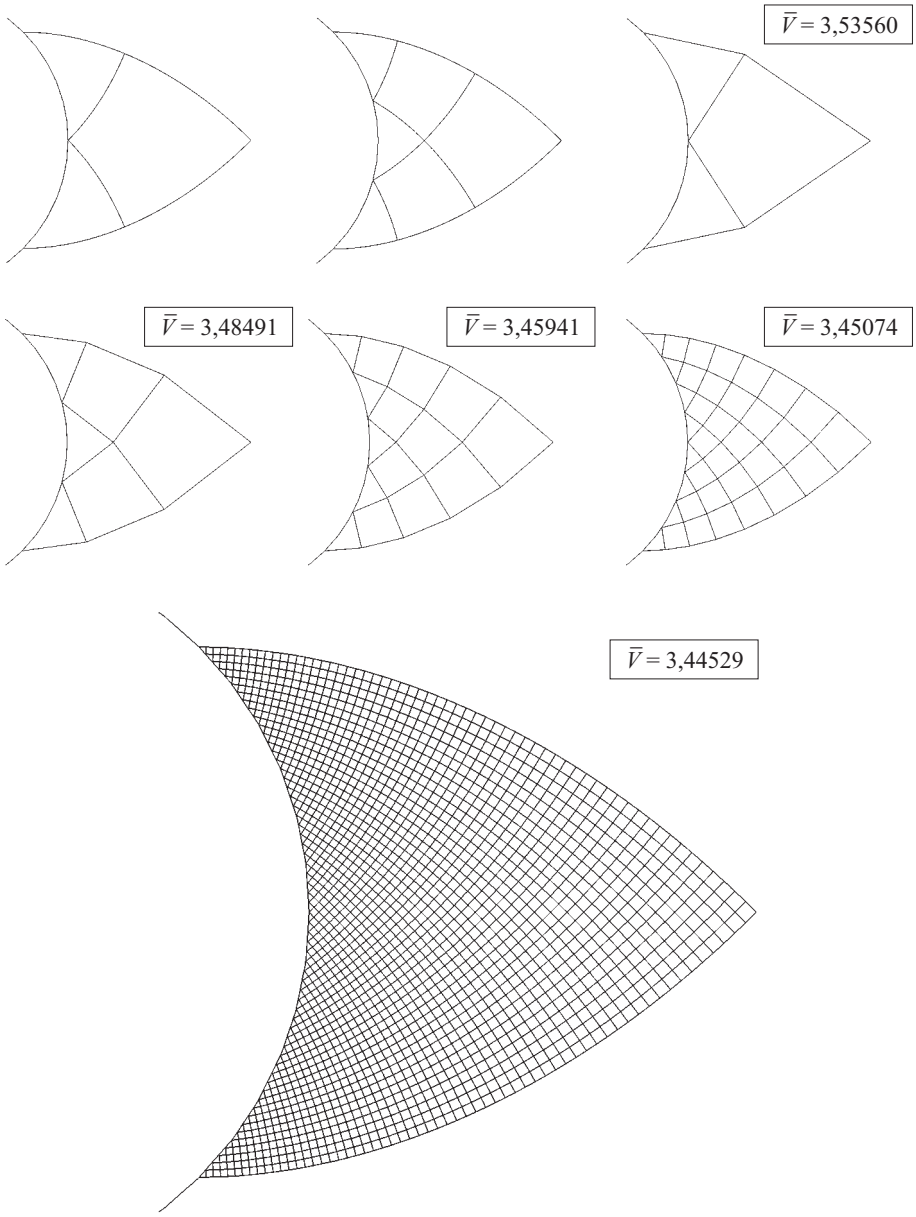

Figure 12. Sequence of trusses supported on one quarter of the circumference of the support. The first two figures show the auxiliary Hencky nets

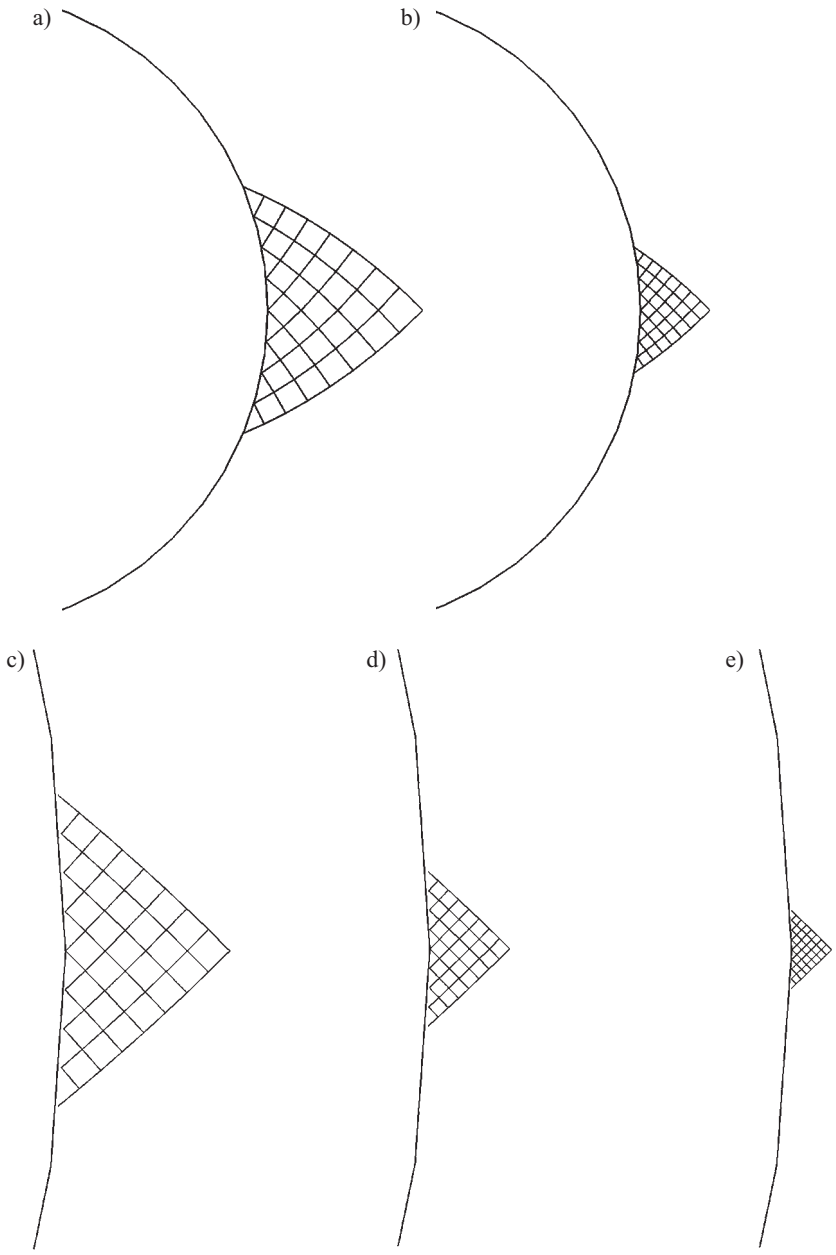

Figure 13. Sequence of trusses corresponding to the diminishing value of the ratio r_p/R; $\alpha_p = \beta_p$ is equal to: a) $\pi/16$, b) $\pi/32$, c) $\pi/64$, d) $\pi/128$, e) $\pi/256$

The angle ϕ_p is measured here in a clockwise direction. Next we proceed as in Section 2. Having found the longitudinal internal forces in the ribs one can compute the force fields $T_1(\alpha,\beta)$ and $T_2(\alpha,\beta)$ within the fibrous domain by applying the Riemann formula (25). The volume of the structure can be computed by (49) to find

$$V = -\frac{2PR}{\sigma_{pl}} e^{\alpha_p+\beta_p}(\alpha_p+\beta_p)\cos(\theta-\phi_p)\ . \tag{59}$$

Let us remind that the coordinates α_p and β_p are negative within the circle, hence the formula (59) gives positive values of the volume. If the load is in the vicinity of the circumference, the optimal structure assumes the form similar to the elementary two-bar design. If the point of application of the load moves towards the centre of the circle the optimal structure acquires more and more bars and becomes supported on longer parts of the circumference, see Fig. 14.

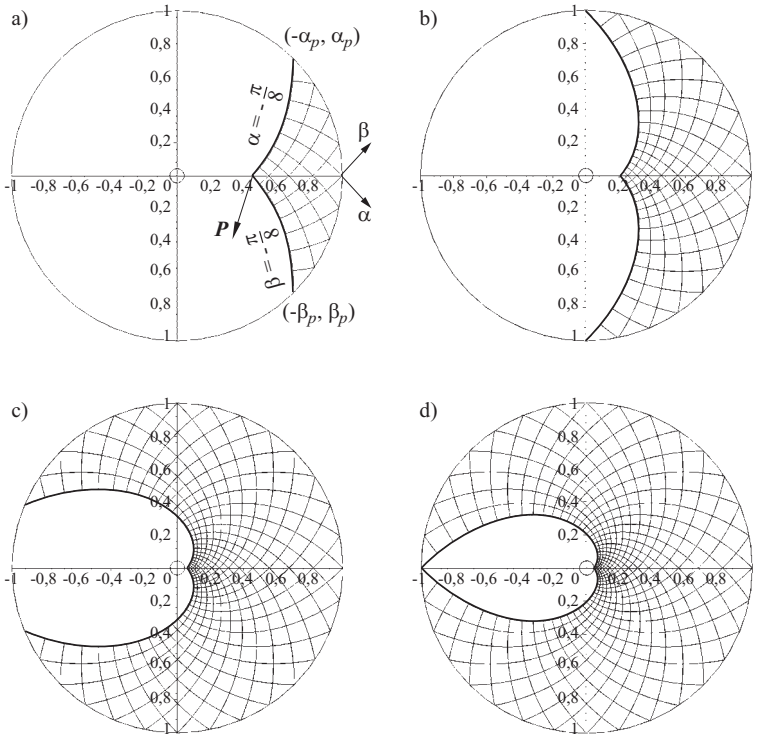

Figure 14. Optimal structure carrying a point load applied inside the circle: a) $\alpha_p = \beta_p = -\pi/8$, b) $\alpha_p = \beta_p = -\pi/4$, c) $\alpha_p = \beta_p = -7\pi/16$, d) $\alpha_p = \beta_p = -\pi/2$

If the distance from the application of the point load to the centre of the circle equals $r = 0.043R$ (which corresponds to $\alpha_p = \beta_p = -\pi/2$ in polar coordinates) the optimal structure becomes supported along the whole circumference. If the distance to the center is smaller, the ribs intersect within the circular domain and the solution considered here ceases to hold. The structure of the greatest volume corresponds to the point of application of the force of coordinates $\alpha_p + \beta_p = -1$; $r = R/e$. This volume is equal

$$V = \frac{2PR}{\sigma_{pl} e} \cos(\theta - \phi_p) \ .$$

Although the geometry of the solution considered here differs from that corresponding to the case of the force outside the circle, the formulae for the volumes of the ribs and the fibrous domain hold here, i.e. the formulae (34)÷(39). Moreover, the previously mentioned relations between the volumes of the fibrous domain and the ribs hold good.

4. Optimal wheel

Consider the problem of finding the lightest structure transmitting a tangent loading of intensity q, distributed along the circumference of the given circle of radius l, to a circular support of radius R. To solve this problem the Hencky net considered in Section 2 is helpful, see Fig. 2. The displacement field (54) is valid here. This field is kinematically admissible since it vanishes along the support. To find the stress resultants we assume that the only component is the shear component $N_{r\theta}$. It satisfies the following equilibrium equation

$$\frac{dN_{r\theta}}{dr} + \frac{2}{r} N_{r\theta} = 0 \ . \tag{60}$$

Its solution, satisfying the given boundary condition: $N_{r\theta}(l) = q$, is expressed by

$$N_{r\theta} = q \left(\frac{l}{r} \right)^2 \ . \tag{61}$$

Thus the principal values of $\boldsymbol{N}$ are: $N_I = N_{r\theta}$, $N_{II} = -N_{r\theta}$. Since the distribution of the function h is given by $h = (|N_I| + |N_{II}|)/\sigma_{pl}$ we find

$$h(r) = \frac{2N_{r\theta}}{\sigma_{pl}} \ . \tag{62}$$

The total volume equals

$$V = \int_R^l \int_0^{2\pi} \frac{2}{\sigma_{pl}} N_{r\theta} r dr d\varphi = \frac{4\pi l^2 q}{\sigma_{pl}} \ln \left(\frac{l}{R} \right) \ . \tag{63}$$

The same result follows from (49). Indeed, we compute the virtual work of the loading by

$$\sigma_{pl}V = \int_0^{2\pi} q \cdot 2l \ln\left(\frac{l}{R}\right) l d\varphi = 4\pi l^2 q \ln\left(\frac{l}{R}\right) \tag{64}$$

and arrive at the same result (63). The optimal wheel is shown in Fig. 15.

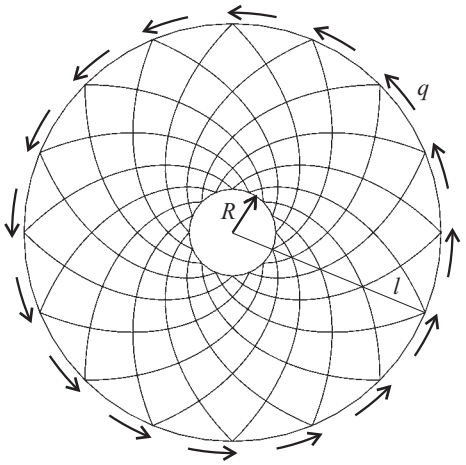

Figure 15. The net of fibres forming an optimal wheel

5. Final remarks

The loading in the form of a point load brings about appearance of ribs in the optimal solution. In the stress-based setting (44) we predict occurence of longitudinal forces within the ribs; these stress resultants are measured in newtons. Such an approach is exact, it assures equivalence of two formulations: (44) and (46). One does not observe singularities of distribution of internal forces T_1, T_2. There is no necessity of replacing the condition $\boldsymbol{\varepsilon}(\boldsymbol{u}) \in \mathbb{B}$ by an integral formula, as has been proposed in Golay and Seppecher (2001, Sec. 3.1). The numerical methods should be formulated such that they comprise plane finite elements as well as bars, or one-dimensional elements.

In the problem of an optimal wheel (Sec. 4) the ribs do not occur, because the loading is distributed along a line. A 3D counterpart of this problem leads to Michells sphere (1904), see Hemp (1973) and Lewiński (2004). The discrete solutions for the Michell sphere can be found in Czarnecki (2003). However, finding a discrete solution close to the exact one is difficult, since the spatial truss formed on a sphere loses its stability, if the number of bars increases.

References

Achtziger, W. (1997) Topology optimization of discrete structures. An introduction in view of computational and non-smooth aspects. In: Rozvany, G.I.N., ed., *Topology Optimization in Structural Mechanics*. Springer, Wien, 57-100.

Allaire, G. and Kohn, R.V. (1993) Optimal design for minimum weight and compliance in plane stress using extremal microstructures. *Eur. J. Mech. A/Solids* **12**, 839-878.

Chan, H.S.Y. (1967) Half-plane slip-line fields and Michell structures. *Q. J. Mech. Appl. Math.* **20**, 453-469.

Chan, H.S.Y. (1975) Symmetric plane frameworks of least weight. In: A. Sawczuk and Z. Mróz, eds., *Optimization in Structural Design*. Springer, Berlin, 313-326.

Cherkaev, A. (2000) *Variational Methods for Structural Optimization*. Springer, New York.

Czarnecki, S. (2003) Compliance optimization of the truss structures. *Comp. Ass. Mech. Eng. Sci.* **10**, 117-137.

Golay, F. and Seppecher, P. (2001) Locking materials and the topology of optimal shapes. *Eur. J. Mech. A/Solids* **20**, 631-644.

Graczykowski, C. and Lewiński, T. (2003) Optimal Michell's cantilever transmitting a given point load to a circular support. Analysis of the exact solution. In: W. Szcześniak, ed., *Theoretical Foundations of Civil Engineering-XI*. Oficyna Wydawnicza PW, Warszawa, 351-368.

Hemp, W.S. (1973) *Optimum Structures*. Oxford, Clarendon Press.

Lewiński, T. (2004) Michell structures formed on surfaces of revolution. *Struct. Multidisc. Optimiz.* **28**, 20-30.

Lewiński, T. and Telega, J.J. (2000) *Plates, laminates and shells. Asymptotic analysis and homogenization*. World Scientific, Singapore, New Jersey, London, Hong Kong.

Lewiński, T. and Telega, J.J. (2001) Michell-like grillages and structures with locking. *Arch. Mech.* **53**, 303-331.

Lewiński, T., Zhou, M. and Rozvany, G.I.N. (1994) Extended exact solutions for least-weight truss layouts – Part I: Cantilever with a horizontal axis of symmetry. *Int. J. Mech. Sci.* **36**, 375-398; Part II: Unsymmetric cantilevers, *Int. J. Mech. Sci.* **36**, 399-419.

Mazurkiewicz, Z.E. (1995) *Thin Elastic Shells*. Oficyna Wydawnicza PW, Warszawa(in Polish).

Michell, A.G.M. (1904) The limits of economy of material in frame structures. *Phil. Mag.* **8**, 589-597.

Novozhilov, V.V. (1970) *Thin Shell Theory*. Walters-Nordhoff, Groningen, Russian Edition: Sudpromgiz, Leningrad 1962.

Rozvany, G.I.N. (1976) *Optimal Design of Flexural Systems: Beams, Grillages, Slabs, Plates and Shells*. Oxford: Pergamon Press.

STRANG, G. and KOHN, R.V. (1983) Hencky-Prandtl nets and constrained Michell trusses. *Comp. Meth. Appl. Mech. Engrg.* **36**, 207-222.

VEKUA, I.N. (1967) New Methods for Solving Elliptic Equations. North-Holland, Amsterdam.

Appendix

The following identities hold

$$\int_{-\alpha_p}^{\beta_p}\int_{-\beta_p}^{\alpha_p} e^{\alpha+\beta}\left[G_1(\beta_p-\beta,\alpha_p-\alpha)-G_1(\alpha_p-\alpha,\beta_p-\beta)\right]d\alpha d\beta = 0 \quad \text{(A.1)}$$

and

$$\mathcal{J}(\alpha_p,\beta_p) = \left[(\alpha_p+\beta_p)-1\right]e^{\alpha_p+\beta_p}+1\ , \quad \text{(A.2)}$$

where $\mathcal{J}(\alpha_p,\beta_p)$ is defined by (33).

Let us denote the l.h.s. of (A.1) by $f(\alpha_p,\beta_p)$. Let us introduce the change of variables

$$\beta_p-\beta = y\ , \qquad \alpha_p-\alpha = x\ . \quad \text{(A.3)}$$

Then

$$f(\alpha_p,\beta_p) = e^{\alpha_p+\beta_p}\int_0^{\alpha_p+\beta_p}\int_0^{\alpha_p+\beta_p-y} e^{-(x+y)}\left[G_1(y,x)-G_1(x,y)\right]dxdy \quad \text{(A.4)}$$

or

$$f(\alpha_p,\beta_p) = e^{\alpha_p+\beta_p}\int_{\Omega_1} e^{-(x+y)}\left[G_1(y,x)-G_1(x,y)\right]d\Omega_1 \quad \text{(A.5)}$$

where Ω_1 is a triangle, see Fig. 16. We note that the $x=y$ axis is the symmetry axis of Ω_1. Therefore $f(\alpha_p,\beta_p)=0$.

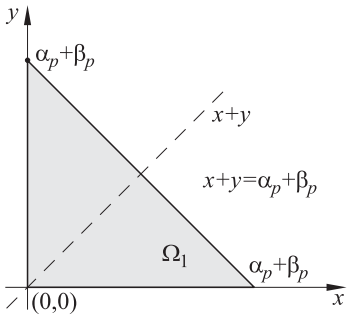

Figure 16. Domain Ω_1 of integration in (A.5)

Let us proceed now to prove (A.2). We apply the change of variables (A.3) and note that $\mathcal{J}(\alpha_p, \beta_p) = j(\alpha_p + \beta_p)$ and

$$e^{-s} j(s) = \int_0^s e^{-y} F(s, y) dy \tag{A.6}$$

with

$$F(s, y) = \int_0^{s-y} e^{-x} \left[G_0(x, y) + G_1(x, y) \right] dx \ . \tag{A.7}$$

Note that

$$\frac{\partial F}{\partial s} = e^{-(s-y)} \left[G_0(s-y, y) + G_1(s-y, y) \right] \ . \tag{A.8}$$

Let us differentiate both sides of (A.6) with respect to s, using (A.8) to find

$$e^s \frac{d}{ds} \left[e^{-s} j(s) \right] = f_1(s) \tag{A.9}$$

where

$$f_1(s) = \int_0^s \left[G_0(s-y, y) + G_1(s-y, y) \right] dy \ . \tag{A.10}$$

We differentiate (A.9) using (22) and $G_0(0, s) = 1$, $G_1(0, s) = 0$ and arrive at

$$\frac{d}{ds} \left\{ e^s \frac{d}{ds} \left(e^{-s} j(s) \right) \right\} = f_1(s) + 1 \tag{A.11}$$

hence

$$\frac{df_1(s)}{ds} = f_1(s) + 1 \tag{A.12}$$

with $f_1(0) = 0$. Thus the function $f_1(s)$ is defined by

$$f_1(s) = e^s - 1 \ . \tag{A.13}$$

We put this result into (A.9) to find

$$e^s \frac{d}{ds} \left(e^{-s} j(s) \right) = e^s - 1 \tag{A.14}$$

hence

$$j(s) = s e^s + 1 + C_1 e^s \tag{A.15}$$

C_1 being a constant. Since $j(0) = 0$ we have $C_1 = -1$, which gives

$$j(s) = s e^s - e^s + 1 \tag{A.16}$$

and this is equivalent to (A.2).